



# What Does PET Imaging Bring to Neuro-Oncology in 2022? A Review

Jules Tianyu Zhang-Yin, Antoine Girard, Marc Bertaux

## ► To cite this version:

Jules Tianyu Zhang-Yin, Antoine Girard, Marc Bertaux. What Does PET Imaging Bring to Neuro-Oncology in 2022? A Review. *Cancers*, 2022, 14 (4), pp.879. 10.3390/cancers14040879 . hal-03660720

**HAL Id: hal-03660720**

**<https://hal.science/hal-03660720>**

Submitted on 6 May 2022

**HAL** is a multi-disciplinary open access archive for the deposit and dissemination of scientific research documents, whether they are published or not. The documents may come from teaching and research institutions in France or abroad, or from public or private research centers.

L'archive ouverte pluridisciplinaire **HAL**, est destinée au dépôt et à la diffusion de documents scientifiques de niveau recherche, publiés ou non, émanant des établissements d'enseignement et de recherche français ou étrangers, des laboratoires publics ou privés.



Distributed under a Creative Commons Attribution 4.0 International License

## Review

# What Does PET Imaging Bring to Neuro-Oncology in 2022? A Review

Jules Tianyu Zhang-Yin <sup>1,\*</sup>, Antoine Girard <sup>2</sup>  and Marc Bertaux <sup>3</sup>

<sup>1</sup> Department of Nuclear Medicine, Clinique Sud Luxembourg, 486762 Arlon, Belgium

<sup>2</sup> Department of Nuclear Medicine, Centre Eugène Marquis, Université Rennes 1, 35000 Rennes, France; a.girard@rennes.unicancer.fr

<sup>3</sup> Department of Nuclear Medicine, Foch Hospital, 92150 Suresnes, France; m.bertaux@hopital-foch.com

\* Correspondence: jules.zhangyin@vivalia.be

**Simple Summary:** Positron emission tomography (PET) imaging is increasingly used to supplement MRI in the management of patient with brain tumors. In this article, we provide a review of the current place and perspectives of PET imaging for the diagnosis and follow-up of from primary brain tumors such as gliomas, meningiomas and central nervous system lymphomas, as well as brain metastases. Different PET radiotracers targeting different biological processes are used to accurately depict these brain tumors and provide unique metabolic and biologic information. Radiolabeled amino acids such as [<sup>18</sup>F]FDOPA or [<sup>18</sup>F]FET are used for imaging of gliomas while both [<sup>18</sup>F]FDG and amino acids can be used for brain metastases. Meningiomas can be seen with a high contrast using radiolabeled ligands of somatostatin receptors, which they usually carry. Unconventional tracers that allow the study of other biological processes such as cell proliferation, hypoxia, or neo-angiogenesis are currently being studied for brain tumors imaging.

**Abstract:** PET imaging is being increasingly used to supplement MRI in the clinical management of brain tumors. The main radiotracers implemented in clinical practice include [<sup>18</sup>F]FDG, radiolabeled amino acids ([<sup>11</sup>C]MET, [<sup>18</sup>F]FDOPA, [<sup>18</sup>F]FET) and [<sup>68</sup>Ga]Ga-DOTA-SSTR, targeting glucose metabolism, L-amino-acid transport and somatostatin receptors expression, respectively. This review aims at addressing the current place and perspectives of brain PET imaging for patients who suffer from primary or secondary brain tumors, at diagnosis and during follow-up. A special focus is given to the following: radiolabeled amino acids PET imaging for tumor characterization and follow-up in gliomas; the role of amino acid PET and [<sup>18</sup>F]FDG PET for detecting brain metastases recurrence; [<sup>68</sup>Ga]Ga-DOTA-SSTR PET for guiding treatment in meningioma and particularly before targeted radiotherapy.

**Keywords:** [<sup>18</sup>F]FDG; [<sup>18</sup>F]FDOPA; [<sup>18</sup>F]FET; [<sup>68</sup>Ga]Ga-DOTA-SSTR; glioma; brain metastases; meningioma; PCNSL



**Citation:** Zhang-Yin, J.T.; Girard, A.; Bertaux, M. What Does PET Imaging Bring to Neuro-Oncology in 2022? A Review. *Cancers* **2022**, *14*, 879. <https://doi.org/10.3390/cancers14040879>

Academic Editor: Marc Brockmann

Received: 31 December 2021

Accepted: 7 February 2022

Published: 10 February 2022

**Publisher's Note:** MDPI stays neutral with regard to jurisdictional claims in published maps and institutional affiliations.



**Copyright:** © 2022 by the authors. Licensee MDPI, Basel, Switzerland. This article is an open access article distributed under the terms and conditions of the Creative Commons Attribution (CC BY) license (<https://creativecommons.org/licenses/by/4.0/>).

## 1. Introduction

Multiparametric magnetic resonance imaging (mpMRI) is the reference method for the diagnosis and follow-up of primary and secondary brain tumors. Nevertheless, its ability to distinguish between viable neoplastic tissue and tumor-free areas is limited in many cases [1–3]. This is especially true in the post-radiation therapy setting where treatment-related changes (TRC) can mimic tumor progression. Over the past few decades, various positron emission tomography (PET) tracers have emerged in the field of neuro-oncology. These radiolabeled molecules can be used as a complementary tool to overcome some of mpMRI's limitations, as follows: to help discriminate TRC changes from tumor progression or relapse, to delineate the tumor extent, to highlight non-enhancing tumors, and to monitor treatment response and to predict the patients' outcome [4,5].

This narrative review aims at addressing the current place and perspectives of brain PET imaging for patients who suffer from primary or secondary brain tumors, at diagnosis and during follow-up. The main clinical applications are as follows: the delineation of tumor extent for treatment planning, assessment of treatment response in gliomas, differential diagnosis and detection of meningioma, distinction of post-therapeutic reactive changes after radiotherapy from progression or recurrence in glioma and brain metastases and differential diagnosis in primary central nervous system lymphoma (PCNSL). The PET tracers involved are  $^{18}\text{F}$ -2-fluoro-2-deoxy-d-glucose ( $^{18}\text{F}$ FDG), radiolabeled amino acids ( $^{11}\text{C}$ methionine ( $^{11}\text{C}$ MET), 3,4-dihydroxy-6- $^{18}\text{F}$ -fluoro-L-phenylalanine ( $^{18}\text{F}$ FDOPA), O-(2- $^{18}\text{F}$  fluoroethyl)-L-tyrosine ( $^{18}\text{F}$ FET)) and  $^{68}\text{Ga}$ [Ga-DOTA-somatostatin receptors (SSTR). A brief look at the emerging aspect of theragnostic, especially for  $^{177}\text{Lu}$ [Lu-DOTA-SSTR in the treatment of meningioma, is also included.

## 2. Tracers

In general oncology,  $^{18}\text{F}$ FDG is a well-established and the most widely used tracer for PET imaging [6]. An increased FDG uptake corresponds to increased glucose metabolism. It is commonly seen in malignancy because of glucose transporter 1 (GLUT1) over-expression and increased hexokinase phosphorylation. Nonetheless, the physiological high FDG uptake in the normal brain, due to neurons' activities, limits the lesion-to-background contrast for brain tumors [5]. Nevertheless,  $^{18}\text{F}$ FDG remains useful for intensely hypermetabolic brain lesions such as PCNSL, glioblastoma and some metastases.

Amino acid PET tracers have the advantage over FDG in that they do not accumulate too much in the normal brain.  $^{11}\text{C}$ MET has been the first developed tracer in this field, but its short half-life (20 min) limits its availability to centers equipped with in-house cyclotron.

Several amino acid PET tracers radiolabeled with  $^{18}\text{F}$  (half-life:110 min) have been developed since then, including  $^{18}\text{F}$ FDOPA and  $^{18}\text{F}$ FET, which are the most often used. Their uptake in brain tumors relies on the overexpression of large amino acid transporters of the L-type (LAT) [7].

Another PET tracer family of interest is  $^{68}\text{Ga}$ -labeled SSTR ligands, since somatostatin receptors are overexpressed in meningioma, with DOTA-D-Phe1-Tyr3-octreotate (DOTATATE) and DOTA-Tyr3-octreotide (DOTATOC) being the most used in clinical routine. They usually require an in-house gallium generator as its half-life is quite short (68 min) but can also be shipped over short distances.

Other PET tracers designed to study various biological aspect of brain tumors have been developed or are currently being developed, but they are still rarely used in clinical routine. It is always important to distinguish radiotracers regarding their ability to cross the healthy blood–brain barrier.  $^{18}\text{F}$ FDG and radiolabeled amino acids ( $^{11}\text{C}$ MET,  $^{18}\text{F}$ FDOPA,  $^{18}\text{F}$ FET) do cross the healthy blood–brain barrier, thus allowing researchers to image infiltrative tumors that do not disrupt it [8,9].

## 3. Glioma

Amino acid PET tracers have relatively high sensitivity for gliomas as the LAT system transporters is overexpressed in most of them [10], with a good tumor-to-background contrast in the brain [11]. Thus, their use has been recommended by the Response Assessment Neuro-Oncology group (RANO) for the assessment of glioma in many situations [5].

### 3.1. Diagnostic and Characterization

$^{11}\text{C}$ MET is chemically equivalent to natural methionine it is incorporated into proteins and could therefore accumulate over time within tumors [12]. Nevertheless,  $^{11}\text{C}$  short physical half-life limits its availability and does not allow for delayed imaging.  $^{11}\text{C}$ MET has good performance to diagnose brain tumors as highlighted in a meta-analysis including more than 400 patients by Zhao et al. [13]. In their study,  $^{11}\text{C}$ MET had a high pooled sensitivity and specificity of 91% and 86% for neoplastic tissue, whereas those of  $^{18}\text{F}$ -FDG were only moderate with sensitivity and specificity of 71% and 77%, respectively.

Nowadays, the emergence of  $^{18}\text{F}$  radiolabeled amino acid tracers such as  $^{18}\text{F}$ FDOPA and  $^{18}\text{F}$ FET enabled a wide use of amino acid PET in clinical practice in many centers. In general, they have comparable diagnostic value compared to  $^{11}\text{C}$ MET [14,15].

$^{18}\text{F}$ FDOPA PET has a good accuracy for the diagnosis of primary brain tumors, with a sensitivity of 96% and a specificity of 86% [16]. It is more specific than  $^{18}\text{F}$ FDG [16] and performs as well as  $^{11}\text{C}$ -MET [17]. The visual and semi-quantitative analyses can both be used. In the visual analysis, the positivity can be defined by a lesion's uptake greater than or equal to striatum uptake. In the semi-quantitative analysis, the only pathology-controlled thresholds to detect brain tumors is a ratio of 1.0 for tumor-to-striatum and 1.3 for tumor-to-brain [16,18] (Figure 1). It can also be used to differentiate high- and low-grade gliomas as the uptake is significantly higher in high-grade gliomas [19]. A recent meta-analysis found a pooled sensitivity of 0.88 and a pooled specificity and 0.73 for glioma grading [20], making it a valuable clinical tool [21]. The dynamic analysis also seems to be an interesting tool to integrate [22–24]. At diagnosis  $^{18}\text{F}$ FDOPA uptake also has an independent prognostic value [25].

In the same line,  $^{18}\text{F}$ FET is another very performant tracer as a meta-analysis of 13  $^{18}\text{F}$ FET PET studies, including more than 450 patients, showed pooled sensitivity and specificity both around 80% for the diagnosis of primary brain tumors [26]. More recently, a second meta-analysis, including 119 patients, reported pooled sensitivity and specificity of 0.94 and 0.88, respectively [27]. A mean tumor-to-background uptake threshold ratio of at least 1.6 and a maximum TBR of at least 2.1 seems to be the best cutoff. Nevertheless, the same authors, in another previous study, have found some contradictory results, especially a relatively low specificity of 62% for a good sensitivity of 84% [26]. The threshold is 2.1 for tumor-to-brain (TBR) max et 1.7 for TBR mean to distinguish glioma versus non-glioma [26]. It allows the biopsy guidance [9] and differentiate efficiently high- and low-grade gliomas, especially thanks to parameters derived from dynamic acquisition [28].

It is particularly important to rule out false positivity, as increased amino acid tracer uptake may also occur in nonneoplastic lesions or inflammatory processes such for  $^{18}\text{F}$ FET and for  $^{18}\text{F}$ FDOPA [29–31], but uptake intensity is generally low or moderate, below the intensity of high-grade gliomas' uptake.

Regarding false negativity, it is mainly related to isocitrate dehydrogenase (IDH)-mutated gliomas. Up to 30% of WHO grade II IDH-mutated gliomas do not show significant amino acid uptake; thus, negative amino acid PET is not sufficient to rule-out low-grade glioma [7,32,33].

### 3.2. Defining Tumor Extent

Delineating glioma extent is important for further diagnostic and therapeutic management, such as biopsy, resection, or radiotherapy planning (Figure 1). To do so  $^{18}\text{F}$ FDOPA and  $^{18}\text{F}$ FET can complement mpMRI. Indeed, conventional mpMRI is particularly limited in its ability to identify non-enhancing glioma subregions [1], whereas  $^{18}\text{F}$ FDOPA PET could discriminate glioma from benign brain lesions such as dysembryoplastic neuroepithelial tumor, and high- from low-grade gliomas, with no contrast enhancement on mpMRI [19]. In a recent biopsy-validated study, molecular information obtained from  $^{18}\text{F}$ FET would reveal a more accurate glioma extent, which is critical for individualized treatment planning [34].

As there is a significant difference in evaluating tumor volume between amino acid PET and mpMRI, it suggests that the latter could substantially underestimate the metabolically active tumor volume [35,36]. Another recent evidence-based article suggested that amino acid PET could improve the delineation of high-grade gliomas compared to standard mpMRI [37]. However, till today, only one study has demonstrated that the management based on amino acid PET-guided benefits a better patient outcome [38].

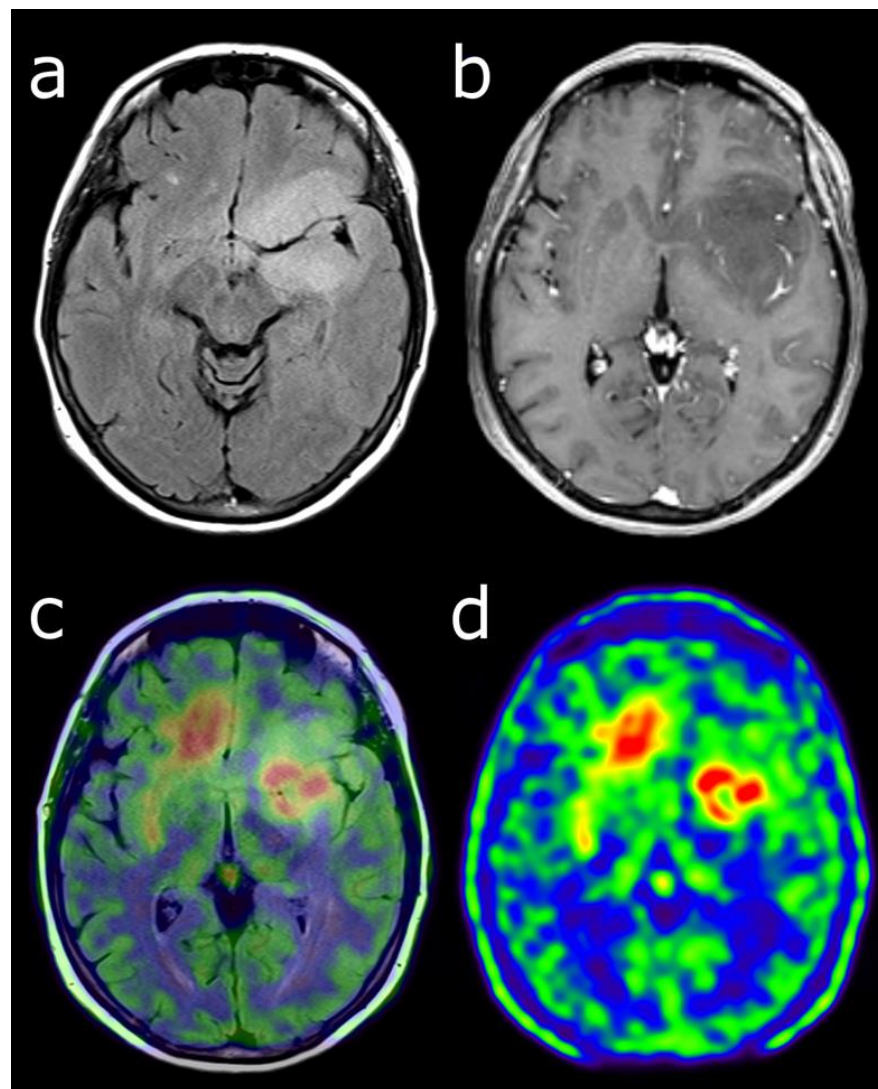


**Figure 1.** Characterization of a left temporo-fronto-insular brain lesion in a 60-year-old woman. This lesion was considered suggestive of grade II or III glioma according T2-FLAIR (a) and post-enhancement T1-weighted MRI (b). [ $^{18}\text{F}$ ]FDOPA PET images (fused with T2-FLAIR MRI (c) and PET only (d)) showed an uptake more intense than twice the normal cortex, predictive of high-grade tumor. Moreover, the lesion visualized with PET was much more extended than with MRI, particularly in the contralateral frontal lobe. Pathological analysis of biopsy samples revealed a WHO grade IV glioblastoma.

### 3.3. Defining Tumor Heterogeneity

The extent of tumor resection is one of the most important prognostic factors in gliomas. Nevertheless, often these tumors are highly heterogeneous with a possible coexistence of high- and low-grade subregions. Thus, presurgical identification of high-grade subregions extent is of major importance. In this very recent biopsy validation study, Girard et al. found that the addition of [ $^{18}\text{F}$ ]FDOPA PET to mpMRI enlarged the delineation volumes and enhanced overall accuracy for detection of high-grade subregions. Thus, combining [ $^{18}\text{F}$ ]FDOPA PET with advanced mpMRI may improve treatment planning in newly diagnosed gliomas [39]. In another clinical trial, better defining tumor heterogeneity seems to have a high impact on radiation therapy. Indeed, [ $^{18}\text{F}$ ]FDOPA PET-guided dose-escalated radiation therapy significantly improved the overall survival in the subgroup of O<sup>6</sup>-methylguanine-DNA methyltransferase (MGMT) methylated glioblastoma patients and the progression-free survival in MGMT unmethylated glioblastoma patients [38].



### 3.4. Monitoring Therapy

In gliomas, frequently used systemic treatment options are alkylating chemotherapy and antiangiogenic therapy, associated with radiotherapy (protocol STUPP). The mpMRI method remains the standard tool for assessment of response but it often lacks specificity [3].

[ $^{18}\text{F}$ ]FET can provide a reliable response assessment after chemotherapy (temozolomide and nitrosourea-based) in patients with high-grade glioma at recurrence [39]. It also can predict patients' outcomes as metabolic responders have better survival [40,41].

An early [ $^{18}\text{F}$ ]FET uptake change, seen 6 weeks after chemoradiotherapy using temozolomide, could already have prognostic information. A decrease in metabolic activity of more than 10% can be a cutoff for predicting better patients' survival [42].

Contrary to [ $^{18}\text{F}$ ]FET, there is less evidence for [ $^{18}\text{F}$ ]FDOPA. There are two studies on assessment after anti-angiogenic treatments, and they concluded that [ $^{18}\text{F}$ ]FDOPA PET could monitor response and identify responders after 2 weeks of treatment with bevacizumab [43,44].

### 3.5. Recurrence vs. Radionecrosis

Differentiating TRC from disease progression is of critical importance for patients' management and prognosis and it can often be challenging [45]. In some countries such as France, suspected recurrent or progressive glioma after treatment is the most common indication for [ $^{18}\text{F}$ ]FDOPA PET in brain tumors. The mpMRI method has some limitations in the case of pseudo-progression in the first 12 weeks after treatment, as in the case of radio-necrosis after 12 weeks of treatment [45,46]. These TRC can appear like a new or increasing contrast enhancement that cannot be distinguished from tumor recurrence.

The [ $^{18}\text{F}$ ]FDOPA PET has an accuracy from 82% to 96% to distinguish TRC vs. a progressive tumor [47,48]. The visual criteria, using the striatum contralateral to the tumor as the reference, or semi-quantitatively, with a tumor-to-striatum ratio of 1.4 for SUVmax and 1.2 for SUV mean, could both be effective [47] (Figure 2).

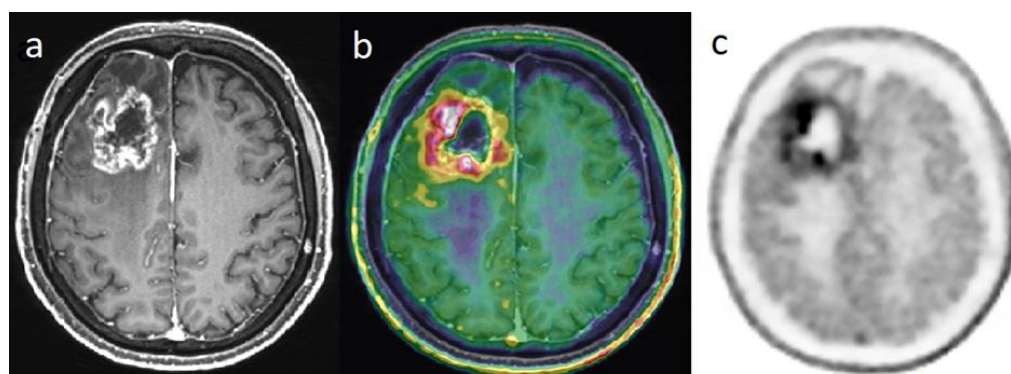


**Figure 2.** Differential diagnosis between recurrence versus radiation necrosis in a 70-year-old man who suffered from a right frontal glioblastoma IDH1-wt and was treated with surgery then chemoradiation with Temodal. Nine months later, there is an increase in edema in the site of the initial tumor. Post-enhancement T1-weighted MRI (a) revealed an increasing contrast enhancement which could correspond to a recurrence or a radionecrosis. [ $^{18}\text{F}$ ]FDOPA PET images (fused with T1-weighted MRI (b) and PET only (c)) showed an intense uptake of this lesion, with tumor/striata ratio = 1.5, suggesting tumor recurrence.

The [ $^{18}\text{F}$ ]FET has a similar performance [44], whereas the [ $^{11}\text{C}$ ]MET encounters a slightly lower accuracy of approximately 75% [49] as MET has more affinity for inflammatory processes [50].

## 4. Metastases

Brain metastases (BM) are the most common malignant brain tumors, as they are part of the natural course of several types of cancer, especially breast and lung cancer, as well

as melanomas. Contrast-enhanced mpMRI is the cornerstone of metastatic brain tumor evaluation. It has widespread availability and excellent spatial resolution, but its specificity can be low, especially in distinguishing TRC from progression, resulting in substantial diagnostic challenges [51]. Amino acid PET tracers can be useful because, as gliomas, metastatic brain tumors overexpress LAT, independently of the primitive tumor. However, [ $^{18}\text{F}$ ]FDG has also a role to play.

#### 4.1. Diagnostic and Characterization

For the detection of BM, the [ $^{18}\text{F}$ ]FDG has poor accuracy, as highlighted in a recent meta-analysis including more than 900 lung cancer patients with brain metastases and comparing contrast-enhanced mpMRI to [ $^{18}\text{F}$ ]FDG PET. It was found that mpMRI has a substantially higher cumulative sensitivity (77%) than [ $^{18}\text{F}$ ]FDG PET (21%) [52].

Amino acid PET tracers are substantially more performant than [ $^{18}\text{F}$ ]FDG, especially for lesions more than 1 cm. Unterrainer et al. reported that [ $^{18}\text{F}$ ]FET were positive for approximately 90% BM, using a ratio  $\geq 1.6$  for tumor/brain [53]. For lesions smaller than 1 cm, the detection rate by mpMRI remains the best, nearly 100% [53]. So, mpMRI is the reference imaging modality for the detection of brain metastases.

There is limited evidence to support the use of PET to distinguish between BM and other brain tumors, especially high-grade glioma [52]. Some authors reported that [ $^{18}\text{F}$ ]FDG is generally lower in metastases than in PCNSL and amino acid PET tracers could identify aggressive tumor features and thus predict a worse prognosis [54,55].

#### 4.2. Detecting Occult Primary Extracerebral Malignancy Revealed by Brain Metastases

In the case of newly discovered BM in patients with no history of cancer, primary lesion and other extracerebral metastases must be sought. Several studies investigating [ $^{18}\text{F}$ ]FDG PET revealed its good performance.

Roh et al. showed that the sensitivity of [ $^{18}\text{F}$ ]FDG PET (87.5%) was significantly higher than that of CT (43.7%) in the detection of the primary tumor in patients with BM [56]. The main sites of other extracerebral metastases are in lymph nodes, especially mediastinal, hilar and retroperitoneal ones [57,58], and the lung was the most frequent primary tumor in patients with brain metastases [58,59]. Moreover, [ $^{18}\text{F}$ ]FDG PET detected additional extracerebral metastatic sites in 42% to 63% of patients [57–60].

#### 4.3. Recurrence vs. Radionecrosis

Among irradiated patients, brain radionecrosis is a common complication, mainly depending on irradiation technique [61], which occurs with an incidence up to 25% [62]. Most of the brain radionecroses are diagnosed during the year after the end of radiotherapy and in 80% within 3 years [63]. Differentiating brain metastases recurrence from radionecrosis can be challenging during mpMRI follow-up after stereotactic radiotherapy.

According to the RANO/PET working group, amino acids PET tracer should be preferred in this indication [51,64]. Reported diagnostic performance of amino acids PET is high and reproducible with sensitivity ranging between 74 and 90% and specificity between 75 and 100% [65–72].

Reported sensitivity of standard [ $^{18}\text{F}$ ]FDG ranges from 40% to 83% and specificity between 50% and 94%, respectively [63,73–75]. This limited diagnostic performance is mainly due to low tumor-to-brain on standard images. To overcome this issue, some authors performed additional delayed PET images 4 to 5 h after [ $^{18}\text{F}$ ]FDG injection. With such protocols, [ $^{18}\text{F}$ ]FDG PET reached sensitivity of 93–95% and specificity of 94–100% [76,77] (Figure 3).

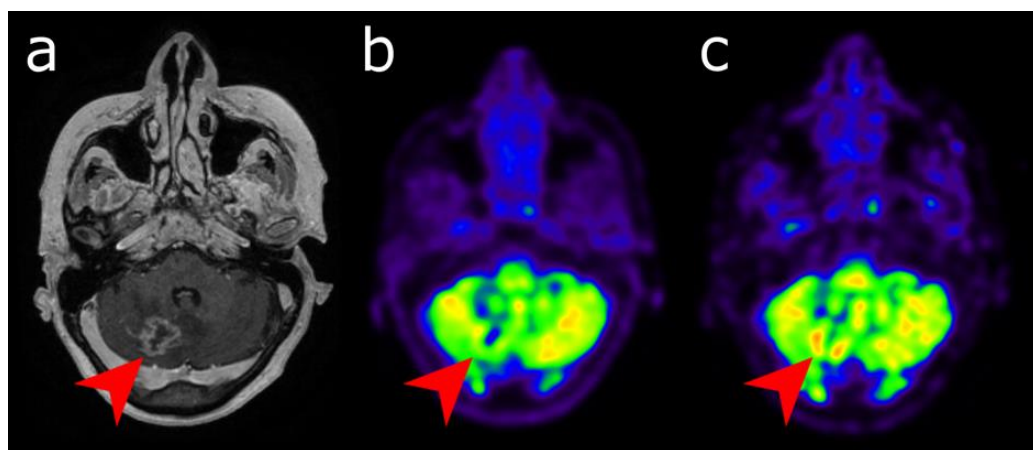


**Figure 3.** Differential diagnosis between recurrence versus radionecrosis in a 73-year-old woman who was treated with stereotactic radiation therapy 2 years earlier for a cerebellar metastasis (red arrow) of breast cancer. Post-enhancement T1-weighted MRI (a) revealed an increasing contrast enhancement. While standard [18F]FDG PET imaging performed 60 min (b) displayed no significant uptake, delayed images performed 4 h post-injection (c) revealed uptake higher than the background activity, suggesting tumor recurrence.

## 5. Meningioma

Meningioma is the most common non-glial primary brain tumor, which represents approximately 35% of all brain tumors. A high SSTR type 2 density is found in all meningioma [78]. [ $^{68}\text{Ga}$ ]Ga-DOTA-SSTR PET tracers are SST analogs with a high binding affinity to SSTR type 2, which make them an effective tool for imaging meningioma.

### 5.1. Diagnostic and Characterization

Detecting meningioma can be challenging using mpMRI, notably when it locates at the skull base or nearby the falx cerebri, often with extension to adjacent bone structure. [ $^{68}\text{Ga}$ ]Ga-DOTA-SSTR has high sensitivity in the detection of meningioma compared to contrast-enhanced mpMRI [79]. Except the pituitary gland, there is no physiological uptake in the brain for [ $^{68}\text{Ga}$ ]Ga-DOTA-SSTR, which provides a high tumor-to-background ratio. The specificity for meningioma is not perfect because [ $^{68}\text{Ga}$ ]Ga-DOTA-SSTR also show a moderate uptake in inflammatory lesions [80]. [ $^{68}\text{Ga}$ ]Ga-DOTA-SSTR PET can be particularly useful for differential diagnosis between meningioma and other kinds of tumors with low SSTR expression, such as schwannoma [81].

### 5.2. Defining Tumor Extent

[ $^{68}\text{Ga}$ ]Ga-DOTA-SSTR PET can delineate more precisely the tumor extent in various tumor locations than contrast-enhanced mpMRI, in a comparative study with histological confirmation [82]. This added value is more pronounced when the tumor is located in regions such as the skull base, orbit and cavernous sinus [83,84] or optic pathway [85]. This is particularly true in meningioma that were previously treated with surgery and/or radiotherapy to differentiate post-therapeutic changes from active meningioma.

Before radiotherapy, it is a valuable tool for improving the GTV (gross tumor volume) and the CTV (clinical target volume) definition and sparing the organs at risk [80].

This optimized target volume delineation is of great help for stereotaxic fractionated radiotherapy in grade I–III meningiomas [86].

In a head-to-head comparison study, [ $^{68}\text{Ga}$ ]Ga-DOTA-SSTR PET performed better than [ $^{18}\text{F}$ ]FET PET in GTV definition. Overall, 2 out of 21 false-negative patients were reported with [ $^{18}\text{F}$ ]FET PET, whereas the [ $^{68}\text{Ga}$ ]Ga-DOTA-SSTR PET had 100% sensitivity [87].



### 5.3. Assessment of Response to Radiotherapy

Only a few data are available in the literature. [ $^{11}\text{C}$ ]MET PET seems to be of interest in the early response assessment after high-energy proton therapy with an average uptake intensity reduction of 19.4% [88]. Ryttefors et al. stated that a follow-up with [ $^{11}\text{C}$ ]MET PET may be a valuable adjunct to, but not a replacement for, standard radiological follow-up [89].

More recently, [ $^{68}\text{Ga}$ ]Ga-DOTA-DOTATATE PET has been proven to be a reliable tool in evaluating treatment responses to radiation therapy. The mean and the maximal total lesion activities decreased significantly with a median of 14.7% [range 8.5–97%] and 36% [range 15–105%], respectively, while the tumor volume based on mpMRI measurement did not change significantly, according to RECIST criteria. Thus, the [ $^{68}\text{Ga}$ ]Ga-DOTA-SSTR PET has incremental value for assessing the treatment response [90].

### 5.4. Diagnosis of Recurrence after Surgery

The recurrence rate is estimated between 20 and 40% within ten years, despite macroscopically complete resection of meningioma [91]. If a sub-total resection has been performed, the recurrence rate for WHO grade I meningiomas could outpass 50% within ten years [92]. The diagnostic accuracy of standard mpMRI is limited, especially in complex situations with bone infiltration or scar tissue. [ $^{68}\text{Ga}$ ]Ga-DOTA-SSTR PET has been proven to add incremental value to mpMRI in the case of TRC [79,82] (Figure 4). It is also useful to differentiate scar tissue from active tumors, with a high sensitivity of 90% [82]. It performs particularly better than mpMRI in the case of transosseous meningiomas, with a sensitivity of 97% and specificity of 100%, compared to 54% and 83%, respectively, for mpMRI [92].

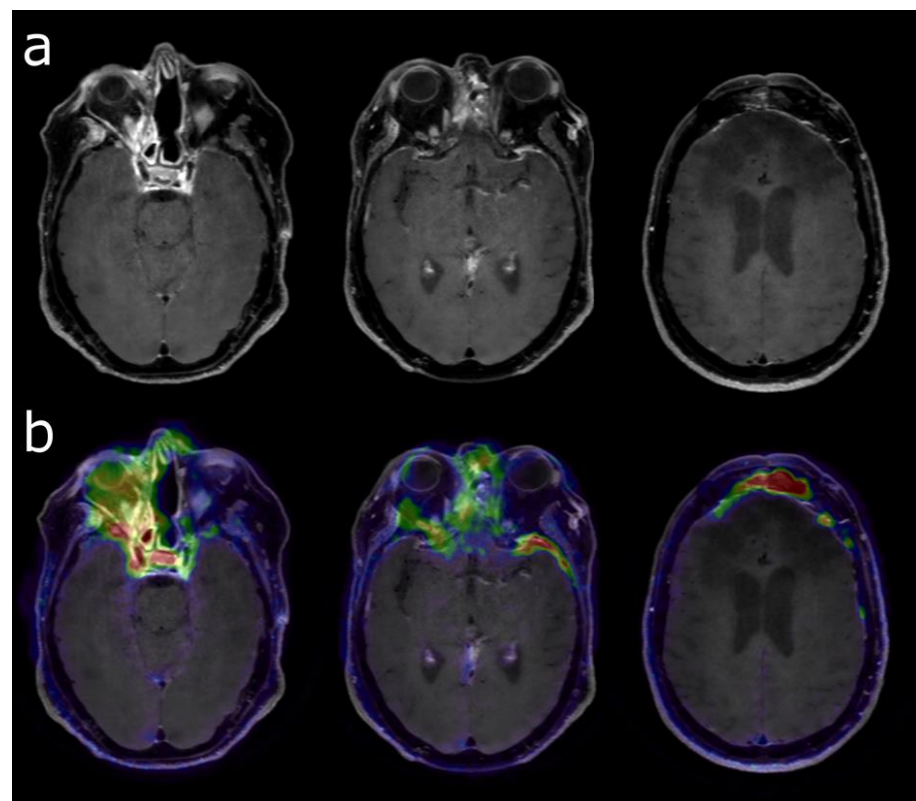


**Figure 4.** Post-enhancement T1-weighted MRI (a) before radiation therapy of a grade 2 skull base meningioma in a 49-year-old woman who was previously treated several times by surgery. [ $^{68}\text{Ga}$ ]Ga-DOTATOC PET (b) was performed to differentiate viable tumor (high uptake) vs. post-therapeutic changes (moderate uptake). Meningioma extension (to frontal and left temporal areas) was much more obvious using [ $^{68}\text{Ga}$ ]Ga-DOTATOC PET in addition to MRI.

### 5.5. [ $^{177}\text{Lu}$ ]Lu-DOTA-SSTR

The prognosis of patients with progressive meningioma after failure of surgery and radiotherapy is poor. Targeted radiation therapy with [ $^{177}\text{Lu}$ ]Lu-DOTA-SSTR, which is well recognized for the treatment of advanced neuroendocrine tumors, is increasingly used for patients with evolving and unresectable meningiomas.

In a phase II clinical trial, Marincek et al. performed 74 treatment cycles on 34 patients, achieving disease stabilization among 23 of them (67%). Stable disease after treatment and high tumor uptake were associated with longer survival [93]. Another retrospective study evaluated the safety and efficacy of [ $^{177}\text{Lu}$ ]Lu-DOTA-SSTR in 20 patients with progressive treatment-refractory meningiomas. The treatment led to disease stabilization in 10 of 20 patients. Median progression-free survivals of 32.2 months for grade I tumors, 7.2 for grade II and 2.1 for grade III were reached. The median overall survival was 17.2 months in grade III patients and not reached for I and II at a median follow-up of 20 months [94]. Finally, in a study including seven patients with progressive intracranial meningioma a progression free survival at six months of 42.9% has been reported after a median of four cycles of  $^{177}\text{Lu}$ -DOTA-SSTR administered, [95].

[ $^{68}\text{Ga}$ ]Ga-DOTA-SSTR PET imaging seems essential before treatment to evaluate the tumor SSTR expression level for individualized treatment optimization.

## 6. PCNSL

PCNSL are non-Hodgkin lymphoma, most frequently represented by diffuse large B-cell lymphoma (DLBCL), confined to the brain, spinal cord, eyes and leptomeninges. Most PCNSL show a very intense [ $^{18}\text{F}$ ]FDG uptake. It can be used for differential diagnosis in both for immunocompetent and immunocompromised patients. In immunocompromised patients, [ $^{18}\text{F}$ ]FDG PET distinguishes correctly PCNSL from other brain infection with a sensibility of 100% and a specificity yielded from 75% to 100% [96]. In immunocompetent patients, [ $^{18}\text{F}$ ]FDG in addition to perfusion MRI enables to differentiate PCNSL from glioblastoma with very good diagnostic accuracy, reaching a sensitivity of 95% and a specificity of 96.4% [97]. The uptake intensity of PCNSL is usually more than twice that of brain physiological uptake [97] (Figure 5).

Concomitant systemic involvement impacts patients' management. [ $^{18}\text{F}$ ]FDG PET has a higher diagnostic yield than computed tomography to detect extracranial lymphoma location and is the imaging method of reference for the staging of systemic DLBCL. Bertaux et al. reported that [ $^{18}\text{F}$ ]FDG PET revealed concomitant occult systemic lymphoma involvement in 8% of 130 PCNSL patients and was more sensitive than a combination of contrast-enhanced CT and bone-marrow biopsy [98]. In a very recent systematic review and meta-analysis, Park et al. stated that whole-body [ $^{18}\text{F}$ ]FDG PET should be preferred over CT in the initial workup of patients with suspected primary CNS lymphoma to detect occult systemic involvement [99].

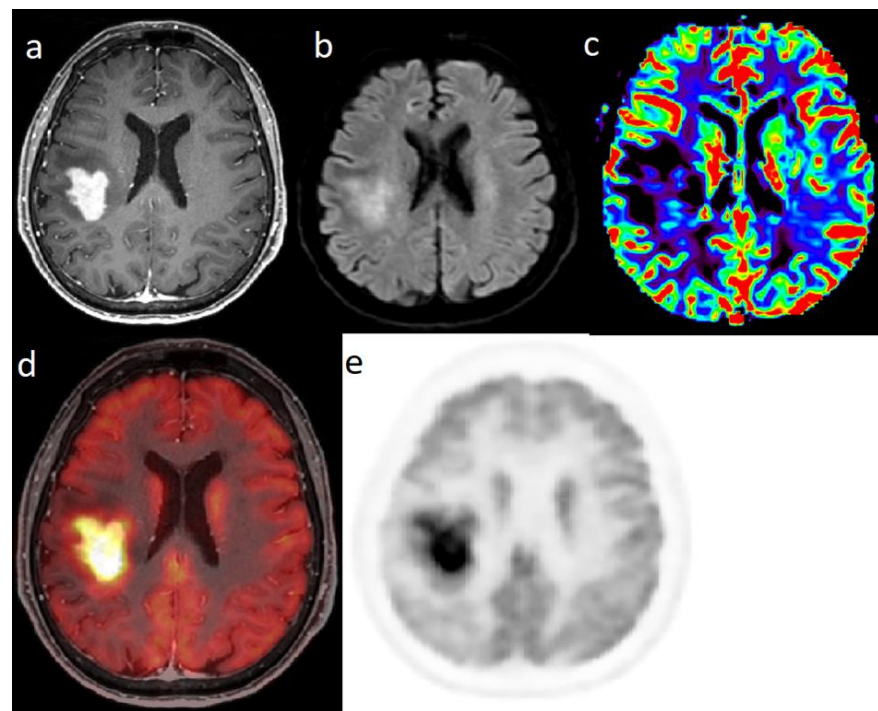


**Figure 5.** Characterization of a single right parietal brain lesion in an 81-year-old woman. Post-enhancement T1-weighted MRI (a) showed an intense increasing contrast enhancement; diffusion weighted imaging (b) showed a hypersignal and there was no hyperperfusion in perfusion-weighted imaging (c). [ $^{18}\text{F}$ ]FDG PET (fused with T1-weighted MRI (d) and PET only (e)) showed a highly intense uptake:  $\text{SUV}_{\text{max}} = 37$ . Pathological analysis of biopsy samples confirmed a PCNSL (type DLBCL).

## 7. Other Aspects of PET Imaging

### 7.1. “Unconventional” Tracers

Numerous innovative PET tracers have been (and are still continuously) developed that target several biological aspects of brain tumors and their micro-environment, as follows: blood flow, angiogenesis, hypoxia, neuroinflammation, mitotic activity and receptor binding [100]. Notably, perfusion can be assessed by [ $^{15}\text{O}$ ]H $_2$ O and [ $^{13}\text{N}$ ]NH $_3$ ; neoangiogenesis can be highlighted by Arg-Gly-Asp peptide (RGD)-based PET tracers, especially [ $^{18}\text{F}$ ]FPPRGD2, [ $^{64}\text{Cu}$ ]DOTA-VEGF121 and [ $^{89}\text{Zr}$ ]Bevacizumab; neuroinflammation can be explored by multiple tracers targeting translocator protein (TSPO), mitotic activity can be revealed by [ $^{18}\text{F}$ ]Fluorothymidine (FLT); and several tracers specifically receptors such as C-X-C chemokine receptor type 4 (CXCR4), epidermal growth factor receptor (EGFR), transforming growth factor- $\beta$  (TGF- $\beta$ ), fibroblast activation protein (FAP) and pyruvate kinase M2 (PKM2) [100].

In clinical practice, [ $^{18}\text{F}$ ]Fluorocholine (FCH) PET can be useful on a case-by-case for tumor characterization and differential diagnosis [81], even though it does not cross the intact blood–brain barrier. Alongi et al. reported a case in which [ $^{18}\text{F}$ ]FCH PET/CT had successively made differential diagnosis between cystic glioblastoma and intraparenchymal hemorrhage, supporting the potential use of this imaging biomarker in surgical or radio-surgical approach [101].

### 7.2. PET/MRI

Integrated PET/MRI systems have been increasingly used in expert centers in recent years. Such systems can provide a complete quick and accurate tumor evaluation by the synchronous acquisition of complementary modalities and thus reduce transportations of patients and increase their comfort. Nevertheless, since these high-end systems remain very expensive, and brain images can be perfectly fused after being acquired separately,

the highest added value of integrated PET/MRI systems is yet limited to clinical research for many brain tumor types [102–104].

### 7.3. Additional Approaches in Image Analysis

Artificial intelligence (AI) has already become a reality in radiology. Since September 2020, the U.S. Centers for Medicare and Medicaid Services officially granted their first reimbursement of a radiology AI algorithm. We can reasonably expect a broader coverage of imaging AI software in clinical practice, including in nuclear medicine. In neuro-oncology, several studies concerning machine learning algorithms and radiomics have already been published, with encouraging results. For example, Russo et al. have developed a predictive model using machine learning based on radiomics, for discriminating between low-grade and high-grade CNS tumors in 56 patients who underwent [ $^{11}\text{C}$ ]MET PET [105]. Kebir et al. highlighted the potential use of radiomics on [ $^{18}\text{F}$ ]FET PET imaging to differentiate multiple sclerosis from glioma, and they concluded that machine learning can enhance lesions classification [106]. Qian et al. used radiomics features extracted from [ $^{18}\text{F}$ ]FDOPA PET to predict methylation of the O6-methylguanine methyltransferase (MGMT) gene promoter status in gliomas, with reasonable accuracy (nearly 80%) [107].

## 8. Conclusions

Molecular imaging with PET, can be of great value in the clinical management of primary and secondary brain tumors, especially as precision and personalized medicine continues to develop. The existing literature provides strong evidence that PET can efficiently supplement MRI in specific settings such as distinguishing recurrence from TRC in glioma and brain metastases. Beyond amino acid PET tracers for glioma, [ $^{68}\text{Ga}$ ]Ga-DOTA-SSTR PET and [ $^{18}\text{F}$ ]FDG PET can play an essential role in the workup of meningiomas, metastases and PCNSL. These diagnostic procedures directly lead to benefits for patients suffering from brain tumors and could be more widely used in clinical routine as the availability of both tracers and imaging systems improves. When appropriately combined with mpMRI, PET imaging has been shown to be of incremental value at many time points in the course of several brain tumors, covering almost the whole diagnostic range in clinical neuro-oncology. Studies are still needed to strengthen the evidence level, specify its exact role in the different scenarios of clinical routine, homogenize practices and provide the community with clear guidelines to systematically implement PET imaging in neuro-oncology.

**Author Contributions:** Conceptualization, J.T.Z.-Y., A.G. and M.B.; methodology, J.T.Z.-Y., A.G. and M.B.; writing—original draft preparation, J.T.Z.-Y., A.G. and M.B.; writing—review and editing, J.T.Z.-Y., A.G. and M.B.; supervision, J.T.Z.-Y. All authors have read and agreed to the published version of the manuscript.

**Funding:** This research received no external funding.

**Conflicts of Interest:** The authors declare no conflict of interest.

## Abbreviations

mp-MRI	multiparametric-magnetic resonance imaging
PET	various positron emission tomography
PCNSL	primary central nervous system lymphoma
[ $^{18}\text{F}$ ]FDG	$^{18}\text{F}$ -2-fluoro-2-deoxy-d-glucose
[ $^{11}\text{C}$ ]MET	[ $^{11}\text{C}$ ]methionine
[ $^{18}\text{F}$ ]FDOPA	3,4-dihydroxy-6- $^{18}\text{F}$ -fluoro-L-phenylalanine
[ $^{18}\text{F}$ ]FET	O-(2- $^{18}\text{F}$ fluoroethyl)
SSTR	somatostatin receptors
GLUT1	glucose transporter 1



LAT	transporters of the L-type
DOTATATE	DOTA-D-Phe1-Tyr3-octreotate
DOTATOC	DOTA-Tyr3-octreotide
FLT	3'-deoxy-3'- <sup>18</sup> F-fluorothymidine
Fluciclovine	anti-1-amino-3- <sup>18</sup> F-fluorocyclobutane-1-carboxylic acid
RANO	Response Assessment Neuro-Oncology group
TRC	treatment-related changes

## References

- Langen, K.J.; Galldiks, N.; Hattingen, E.; Shah, N.J. Advances in neuro-oncology imaging. *Nat. Rev. Neurol.* **2017**, *13*, 279–289. [\[CrossRef\]](#) [\[PubMed\]](#)
- Pope, W.B.; Brandal, G. Conventional and advanced magnetic resonance imaging in patients with high-grade glioma. *Q. J. Nucl. Med. Mol. Imaging* **2018**, *62*, 239–253. [\[CrossRef\]](#) [\[PubMed\]](#)
- Dhermain, F.G.; Hau, P.; Lanfermann, H.; Jacobs, A.H.; van den Bent, M.J. Advanced MRI and PET imaging for assessment of treatment response in patients with gliomas. *Lancet Neurol.* **2010**, *9*, 906–920. [\[CrossRef\]](#)
- Langen, K.J.; Watts, C. Neuro-Oncology: Amino acid PET for brain tumours—Ready for the clinic? *Nat. Rev. Neurol.* **2016**, *12*, 375–376. [\[CrossRef\]](#) [\[PubMed\]](#)
- Albert, N.; Weller, M.; Suchorska, B.; Galldiks, N.; Soffietti, R.; Kim, M.; la Fougère, C.; Pope, W.; Law, I.; Arbizu, J.; et al. Response Assessment in Neuro-Oncology working group and European Association for Neuro-Oncology recommendations for the clinical use of PET imaging in gliomas. *Neuro Oncol.* **2016**, *18*, 1199–1208. [\[CrossRef\]](#) [\[PubMed\]](#)
- Herholz, K.; Langen, K.; Schiepers, C.; Mountz, J. Brain Tumors. *Semin. Nucl. Med.* **2012**, *42*, 356–370. [\[CrossRef\]](#) [\[PubMed\]](#)
- Hutterer, M.; Nowosielski, M.; Putzer, D.; Jansen, N.; Seiz, M.; Schocke, M.; McCoy, M.; Göbel, G.; la Fougère, C.; Virgolini, I.; et al. [<sup>18</sup>F]-fluoro-ethyl-L-tyrosine PET: A valuable diagnostic tool in neuro-oncology, but not all that glitters is glioma. *Neuro Oncol.* **2013**, *15*, 341–351. [\[CrossRef\]](#)
- Pauleit, D.; Stoffels, G.; Schaden, W.; Hamacher, K.; Bauer, D.; Tellmann, L.; Herzog, H.; Bröer, S.; Coenen, H.H.; Langen, K.J. PET with O-(2-<sup>18</sup>F-Fluoroethyl)-L-Tyrosine in peripheral tumors: First clinical results. *J. Nucl. Med.* **2005**, *46*, 411–416.
- Pauleit, D.; Floeth, F.; Hamacher, K.; Riemenschneider, M.J.; Reifenberger, G.; Müller, H.W.; Zilles, K.; Coenen, H.H.; Langen, K.J. O-(2-[<sup>18</sup>F]fluoroethyl)-L-tyrosine PET combined with MRI improves the diagnostic assessment of cerebral gliomas. *Brain* **2005**, *128*, 678–687. [\[CrossRef\]](#)
- Papin-Michault, C.; Bonnetaud, C.; Dufour, M.; Almairac, F.; Coutts, M.; Patouraux, S.; Virolle, T.; Darcourt, J.; Burel-Vandenbos, F. Study of LAT1 Expression in Brain Metastases: Towards a Better Understanding of the Results of Positron Emission Tomography Using Amino Acid Tracers. *PLoS ONE* **2016**, *11*, e0157139. [\[CrossRef\]](#)
- Wester, H.; Herz, M.; Weber, W.; Heiss, P.; Senekowitsch-Schmidtke, R.; Schwaiger, M.; Stöcklin, G. Synthesis and radiopharmacology of O-(2-[<sup>18</sup>F]fluoroethyl)-L-tyrosine for tumor imaging. *J. Nucl. Med.* **1999**, *40*, 205–212. [\[PubMed\]](#)
- Borbély, K.; Nyáry, I.; Tóth, M.; Ericson, K.; Gulyás, B. Optimization of semi-quantification in metabolic PET studies with <sup>18</sup>F-fluorodeoxyglucose and <sup>11</sup>C-methionine in the determination of malignancy of gliomas. *J. Neurol. Sci.* **2006**, *246*, 85–94. [\[CrossRef\]](#) [\[PubMed\]](#)
- Zhao, C.; Zhang, Y.; Wang, J. A meta-analysis on the diagnostic performance of (<sup>18</sup>F)-FDG and (<sup>11</sup>C)-methionine PET for differentiating brain tumors. *Am. J. Neuroradiol.* **2013**, *35*, 1058–1065. [\[CrossRef\]](#) [\[PubMed\]](#)
- Grosu, A.; Astner, S.; Riedel, E.; Nieder, C.; Wiedenmann, N.; Heinemann, F.; Schwaiger, M.; Molls, M.; Wester, H.; Weber, W. An interindividual comparison of O-(2-[<sup>18</sup>F]fluoroethyl)-L-tyrosine (FET)- and L-[methyl-<sup>11</sup>C]methionine (MET)-PET in patients with brain gliomas and metastases. *Int. J. Radiat. Oncol. Biol. Phys.* **2011**, *81*, 1049–1058. [\[CrossRef\]](#)
- Janvier, L.; Olivier, P.; Blonski, M.; Morel, O.; Vignaud, J.; Karcher, G.; Taillandier, L.; Verger, A. Correlation of SUV-Derived Indices with Tumoral Aggressiveness of Gliomas in Static <sup>18</sup>F-FDOPA PET: Use in Clinical Practice. *Clin. Nucl. Med.* **2015**, *40*, e429–e435. [\[CrossRef\]](#)
- Chen, W.; Silverman, D.H.; Delaloye, S.; Czernin, J.; Kamdar, N.; Pope, W.; Satyamurthy, N.; Schiepers, C.; Cloughesy, T. <sup>18</sup>F-FDOPA PET imaging of brain tumors: Comparison study with <sup>18</sup>F-FDG PET and evaluation of diagnostic accuracy. *J. Nucl. Med.* **2006**, *47*, 904–911.
- Becherer, A.; Karanikas, G.; Szabó, M.; Zettinig, G.; Asenbaum, S.; Marosi, C.; Henk, C.; Wunderbaldinger, P.; Czech, T.; Wadsak, W.; et al. Brain tumour imaging with PET: A comparison between [<sup>18</sup>F]fluorodopa and [<sup>11</sup>C]methionine. *Eur. J. Nucl. Med. Mol. Imaging* **2003**, *30*, 1561–1567. [\[CrossRef\]](#)
- Lizarraga, K.; Allen-Auerbach, M.; Czernin, J.; DeSalles, A.; Yong, W.; Phelps, M.; Chen, W. (<sup>18</sup>F)-FDOPA PET for differentiating recurrent or progressive brain metastatic tumors from late or delayed radiation injury after radiation treatment. *J. Nucl. Med.* **2013**, *55*, 30–36. [\[CrossRef\]](#)
- Bund, C.; Heimburger, C.; Imperiale, A.; Lhermitte, B.; Chenard, M.; Lefebvre, F.; Kremer, S.; Proust, F.; Namer, I. FDOPA PET-CT of Nonenhancing Brain Tumors. *Clin. Nucl. Med.* **2017**, *42*, 250–257. [\[CrossRef\]](#)
- Xiao, J.; Jin, Y.; Nie, J.; Chen, F.; Ma, X. Diagnostic and grading accuracy of <sup>18</sup>F-FDOPA PET and PET/CT in patients with gliomas: A systematic review and meta-analysis. *BMC Cancer* **2019**, *19*, 767. [\[CrossRef\]](#)



21. Verger, A.; Arbizu, J.; Law, I. Role of amino-acid PET in high-grade gliomas: Limitations and perspectives. *Q. J. Nucl. Med. Mol. Imaging* **2018**, *62*, 254–266. [[CrossRef](#)] [[PubMed](#)]
22. Verger, A.; Kas, A.; Darcourt, J.; Chinot, O.; Taillandier, L.; Hoang Xuan, K.; Guedj, E.; Bouvet, C.; Bund, C.; Guedj, E.; et al. Joint SFMN/ANOCEF focus on 18F-FDOPA PET imaging in glioma: Current applications and perspectives. *Méd. Nucl.* **2020**, *3*, 164–171. [[CrossRef](#)]
23. Girard, A.; Saint-Jalmes, H.; Chaboub, N.; Le Reste, P.J.; Metais, A.; Devillers, A.; Le Jeune, F.; Palard-Novello, X. Optimization of time frame binning for FDOPA uptake quantification in glioma. *PLoS ONE* **2020**, *15*, e0232141. [[CrossRef](#)] [[PubMed](#)]
24. Girard, A.; Le Reste, P.J.; Metais, A.; Chaboub, N.; Devillers, A.; Saint-Jalmes, H.; Jeune, F.L.; Palard-Novello, X. Additive Value of Dynamic FDOPA PET/CT for Glioma Grading. *Front. Med.* **2021**, *8*, 705996. [[CrossRef](#)] [[PubMed](#)]
25. Patel, C.; Fazzari, E.; Chakhoyan, A.; Yao, J.; Raymond, C.; Nguyen, H.; Manoukian, J.; Nguyen, N.; Pope, W.; Cloughesy, T.; et al. 18F-FDOPA PET and MRI characteristics correlate with degree of malignancy and predict survival in treatment-naïve gliomas: A cross-sectional study. *J. Neurooncol.* **2018**, *139*, 399–409. [[CrossRef](#)]
26. Dunet, V.; Rossier, C.; Buck, A.; Stupp, R.; Prior, J. Performance of 18F-fluoro-ethyl-tyrosine (18F-FET) PET for the differential diagnosis of primary brain tumor: A systematic review and Metaanalysis. *J. Nucl. Med.* **2012**, *53*, 207–214. [[CrossRef](#)]
27. Dunet, V.; Pomoni, A.; Hottinger, A.; Nicod-Lalonde, M.; Prior, J. Performance of 18F-FET versus 18F-FDG-PET for the diagnosis and grading of brain tumors: Systematic review and meta-analysis. *Neuro Oncol.* **2015**, *18*, 426–434. [[CrossRef](#)] [[PubMed](#)]
28. Pöpperl, G.; Kreth, F.; Mehrkens, J.; Herms, J.; Seelos, K.; Koch, W.; Gildehaus, F.; Kretzschmar, H.; Tonn, J.; Tatsch, K. FET PET for the evaluation of untreated gliomas: Correlation of FET uptake and uptake kinetics with tumour grading. *Eur. J. Nucl. Med. Mol. Imaging* **2007**, *34*, 1933–1942. [[CrossRef](#)]
29. Pichler, R.; Dunzinger, A.; Wurm, G.; Pichler, J.; Weis, S.; Nußbaumer, K.; Topakian, R.; Aigner, R. Is there a place for FET PET in the initial evaluation of brain lesions with unknown significance? *Eur. J. Nucl. Med. Mol. Imaging* **2010**, *37*, 1521–1528. [[CrossRef](#)]
30. Calabria, F.F.; Chiaravalloti, A.; Jaffrain-Rea, M.L.; Zinzi, M.; Sannino, P.; Minniti, G.; Rubello, D.; Schillaci, O. 18F-DOPA PET/CT Physiological Distribution and Pitfalls: Experience in 215 Patients. *Clin. Nucl. Med.* **2016**, *41*, 753–760. [[CrossRef](#)]
31. Sala, Q.; Metellus, P.; Taieb, D.; Kaphan, E.; Figarella-Branger, D.; Guedj, E. 18F-DOPA, a clinically available PET tracer to study brain inflammation? *Clin. Nucl. Med.* **2014**, *39*, e283–e285. [[CrossRef](#)]
32. Jansen, N.; Graute, V.; Armbruster, L.; Suchorska, B.; Lutz, J.; Eigenbrod, S.; Cumming, P.; Bartenstein, P.; Tonn, J.; Kreth, F.; et al. MRI-Suspected low-grade glioma: Is there a need to perform dynamic FET PET? *Eur. J. Nucl. Med. Mol. Imaging* **2012**, *39*, 1021–1029. [[CrossRef](#)] [[PubMed](#)]
33. Suchorska, B.; Giese, A.; Biczok, A.; Unterrainer, M.; Weller, M.; Drexler, M.; Bartenstein, P.; Schüller, U.; Tonn, J.; Albert, N. Identification of time-to-peak on dynamic 18F-FET-PET as a prognostic marker specifically in IDH1/2 mutant diffuse astrocytoma. *Neuro Oncol.* **2017**, *20*, 279–288. [[CrossRef](#)]
34. Song, S.; Cheng, Y.; Ma, J.; Wang, L.; Dong, C.; Wei, Y.; Xu, G.; An, Y.; Qi, Z.; Lin, Q.; et al. Simultaneous FET-PET and contrast-enhanced MRI based on hybrid PET/MR improves delineation of tumor spatial biodistribution in gliomas: A biopsy validation study. *Eur. J. Nucl. Med. Mol. Imaging* **2020**, *47*, 1458–1467. [[CrossRef](#)]
35. Lohmann, P.; Werner, J.; Shah, N.; Fink, G.; Langen, K.; Galldiks, N. Combined Amino Acid Positron Emission Tomography and Advanced Magnetic Resonance Imaging in Glioma Patients. *Cancers* **2019**, *11*, 153. [[CrossRef](#)] [[PubMed](#)]
36. Kunz, M.; Thon, N.; Eigenbrod, S.; Hartmann, C.; Egensperger, R.; Herms, J.; Geisler, J.; la Fougere, C.; Lutz, J.; Linn, J.; et al. Hot spots in dynamic (18)FET-PET delineate malignant tumor parts within suspected WHO grade II gliomas. *Neuro Oncol.* **2011**, *13*, 307–316. [[CrossRef](#)] [[PubMed](#)]
37. Verburg, N.; Hoefnagels, F.; Barkhof, F.; Boellaard, R.; Goldman, S.; Guo, J.; Heimans, J.; Hoekstra, O.; Jain, R.; Kinoshita, M.; et al. Diagnostic Accuracy of Neuroimaging to Delineate Diffuse Gliomas within the Brain: A Meta-Analysis. *Am. J. Neuroradiol.* **2017**, *38*, 1884–1891. [[CrossRef](#)]
38. Laack, N.; Pafundi, D.; Anderson, S.; Kaufmann, T.; Lowe, V.; Hunt, C.; Vogen, D.; Yan, E.; Sarkaria, J.; Brown, P.; et al. Initial Results of a Phase 2 Trial of <sup>18</sup>F-DOPA PET-Guided Dose-Escalated Radiation Therapy for Glioblastoma. *Int. J. Radiat. Oncol. Biol. Phys.* **2021**, *110*, 1383–1395. [[CrossRef](#)]
39. Galldiks, N.; Kracht, L.; Burghaus, L.; Ullrich, R.; Backes, H.; Brunn, A.; Heiss, W.; Jacobs, A. Patient-Tailored, imaging-guided, long-term temozolomide chemotherapy in patients with glioblastoma. *Mol. Imaging* **2010**, *9*, 40–46. [[CrossRef](#)]
40. Roelcke, U.; Wyss, M.; Nowosielski, M.; Rudà, R.; Roth, P.; Hofer, S.; Galldiks, N.; Crippa, F.; Weller, M.; Soffietti, R. Amino acid positron emission tomography to monitor chemotherapy response and predict seizure control and progression-free survival in WHO grade II gliomas. *Neuro Oncol.* **2015**, *18*, 744–751. [[CrossRef](#)]
41. Suchorska, B.; Unterrainer, M.; Biczok, A.; Sosnova, M.; Forbrig, R.; Bartenstein, P.; Tonn, J.; Albert, N.; Kreth, F. <sup>18</sup>F-FET-PET as a biomarker for therapy response in non-contrast enhancing glioma following chemotherapy. *J. Neurooncol.* **2018**, *139*, 721–730. [[CrossRef](#)]
42. Galldiks, N.; Langen, K.; Holy, R.; Pinkawa, M.; Stoffels, G.; Nolte, K.; Kaiser, H.; Filss, C.; Fink, G.; Coenen, H.; et al. Assessment of treatment response in patients with glioblastoma using O-(2-18F-fluoroethyl)-L-tyrosine PET in comparison to MRI. *J. Nucl. Med.* **2012**, *53*, 1048–1057. [[CrossRef](#)] [[PubMed](#)]
43. Harris, R.; Cloughesy, T.; Pope, W.; Nghiemphu, P.; Lai, A.; Zaw, T.; Czernin, J.; Phelps, M.; Chen, W.; Ellingson, B. 18F-FDOPA and 18F-FLT positron emission tomography parametric response maps predict response in recurrent malignant gliomas treated with bevacizumab. *Neuro Oncol.* **2012**, *14*, 1079–1089. [[CrossRef](#)]

44. Schwarzenberg, J.; Czernin, J.; Cloughesy, T.; Ellingson, B.; Pope, W.; Grogan, T.; Elashoff, D.; Geist, C.; Silverman, D.; Phelps, M.; et al. Treatment response evaluation using 18F-FDOPA PET in patients with recurrent malignant glioma on bevacizumab therapy. *Clin. Cancer Res.* **2014**, *20*, 3550–3559. [\[CrossRef\]](#) [\[PubMed\]](#)
45. Galldiks, N.; Stoffels, G.; Filss, C.; Rapp, M.; Blau, T.; Tscherpel, C.; Ceccon, G.; Dunkl, V.; Weinzierl, M.; Stoffel, M.; et al. The use of dynamic O-(2-18F-fluoroethyl)-L-tyrosine PET in the diagnosis of patients with progressive and recurrent glioma. *Neuro Oncol.* **2015**, *17*, 1293–1300. [\[CrossRef\]](#) [\[PubMed\]](#)
46. Shah, A.; Snelling, B.; Bregy, A.; Patel, P.; Tememe, D.; Bhatia, R.; Sklar, E.; Komotar, R. Discriminating radiation necrosis from tumor progression in gliomas: A systematic review what is the best imaging modality? *J. Neurooncol.* **2013**, *112*, 141–152. [\[CrossRef\]](#)
47. Herrmann, K.; Czernin, J.; Cloughesy, T.; Lai, A.; Pomykala, K.; Benz, M.; Buck, A.; Phelps, M.; Chen, W. Comparison of visual and semiquantitative analysis of 18F-FDOPA-PET/CT for recurrence detection in glioblastoma patients. *Neuro Oncol.* **2013**, *16*, 603–609. [\[CrossRef\]](#)
48. Karunanithi, S.; Sharma, P.; Kumar, A.; Khangembam, B.; Bandopadhyaya, G.; Kumar, R.; Gupta, D.; Malhotra, A.; Bal, C. 18F-FDOPA PET/CT for detection of recurrence in patients with glioma: Prospective comparison with 18F-FDG PET/CT. *Eur. J. Nucl. Med. Mol. Imaging* **2013**, *40*, 1025–1035. [\[CrossRef\]](#)
49. Nishashi, T.; Dahabreh, I.J.; Terasawa, T. Diagnostic accuracy of PET for recurrent glioma diagnosis: A meta-analysis. *Am. J. Neuroradiol.* **2013**, *34*, 944–950. [\[CrossRef\]](#)
50. Salber, D.; Stoffels, G.; Pauleit, D.; Oros-Peusquens, A.; Shah, N.; Klauth, P.; Hamacher, K.; Coenen, H.; Langen, K. Differential uptake of O-(2-18F-fluoroethyl)-L-tyrosine, L-3H-methionine, and 3H-deoxyglucose in brain abscesses. *J. Nucl. Med.* **2007**, *48*, 2056–2062. [\[CrossRef\]](#) [\[PubMed\]](#)
51. Galldiks, N.; Langen, K.; Albert, N.; Chamberlain, M.; Soffietti, R.; Kim, M.; Law, I.; Le Rhun, E.; Chang, S.; Schwarting, J.; et al. PET imaging in patients with brain metastasis-report of the RANO/PET group. *Neuro Oncol.* **2019**, *21*, 585–595. [\[CrossRef\]](#)
52. Li, Y.; Jin, G.; Su, D. Comparison of gadolinium-enhanced MRI and 18FDG PET/PET-CT for the diagnosis of brain metastases in lung cancer patients: A meta-analysis of 5 prospective studies. *Oncotarget* **2017**, *8*, 35743–35749. [\[CrossRef\]](#) [\[PubMed\]](#)
53. Unterrainer, M.; Galldiks, N.; Suchorska, B.; Kowalew, L.; Wenter, V.; Schmid-Tannwald, C.; Niyazi, M.; Bartenstein, P.; Langen, K.; Albert, N. <sup>18</sup>F-FET PET Uptake Characteristics in Patients with Newly Diagnosed and Untreated Brain Metastasis. *J. Nucl. Med.* **2016**, *58*, 584–589. [\[CrossRef\]](#) [\[PubMed\]](#)
54. Kaira, K.; Oriuchi, N.; Imai, H.; Shimizu, K.; Yanagitani, N.; Sunaga, N.; Hisada, T.; Tanaka, S.; Ishizuka, T.; Kanai, Y.; et al. Prognostic significance of L-type amino acid transporter 1 expression in resectable stage I-III nonsmall cell lung cancer. *Br. J. Cancer* **2008**, *98*, 742–748. [\[CrossRef\]](#)
55. Yanagisawa, N.; Ichino, M.; Mikami, T.; Nakada, N.; Hana, K.; Koizumi, W.; Endou, H.; Okayasu, I. High expression of L-type amino acid transporter 1 (LAT1) predicts poor prognosis in pancreatic ductal adenocarcinomas. *J. Clin. Pathol.* **2012**, *65*, 1019–1023. [\[CrossRef\]](#) [\[PubMed\]](#)
56. Roh, J.; Kim, J.; Lee, J.; Cho, K.; Choi, S.; Nam, S.; Kim, S. Utility of combined (18)F-fluorodeoxyglucose-positron emission tomography and computed tomography in patients with cervical metastases from unknown primary tumors. *Oral Oncol.* **2009**, *45*, 218–224. [\[CrossRef\]](#)
57. Wolpert, F.; Weller, M.; Berghoff, A.; Rushing, E.; Füreder, L.; Petyt, G.; Leske, H.; Andratschke, N.; Regli, L.; Neidert, M.; et al. Diagnostic value of <sup>18</sup>F-fluorodeoxyglucose positron emission tomography for patients with brain metastasis from unknown primary site. *Eur. J. Cancer* **2018**, *96*, 64–72. [\[CrossRef\]](#) [\[PubMed\]](#)
58. Koç, Z.P.; Kara, P.Ö.; Dağtekin, A. Detection of unknown primary tumor in patients presented with brain metastasis by F-18 fluorodeoxyglucose positron emission tomography/computed tomography. *CNS Oncol.* **2018**, *7*, 12. [\[CrossRef\]](#)
59. Cengiz, A.; Göksel, S.; Yürekli, Y. Diagnostic Value of <sup>18</sup>F-FDG PET/CT in Patients with Carcinoma of Unknown Primary. *Mol. Imaging Radionucl. Ther.* **2018**, *27*, 126–132. [\[CrossRef\]](#)
60. Mohamed, D.M.; Kamel, H.A. Diagnostic efficiency of PET/CT in patients with cancer of unknown primary with brain metastasis as initial manifestation and its impact on overall survival. *Egypt J. Radiol. Nucl. Med.* **2021**, *52*, 65–70. [\[CrossRef\]](#)
61. Ruben, J.; Dally, M.; Bailey, M.; Smith, R.; McLean, C.; Fedele, P. Cerebral radiation necrosis: Incidence, outcomes, and risk factors with emphasis on radiation parameters and chemotherapy. *Int. J. Radiat. Oncol. Biol. Phys.* **2006**, *65*, 499–508. [\[CrossRef\]](#) [\[PubMed\]](#)
62. Vellayappan, B.; Tan, C.; Yong, C.; Khor, L.; Koh, W.; Yeo, T.; Detsky, J.; Lo, S.; Sahgal, A. Diagnosis and Management of Radiation Necrosis in Patients with Brain Metastases. *Front. Oncol.* **2018**, *28*, 395. [\[CrossRef\]](#) [\[PubMed\]](#)
63. Walker, A.; Ruzevick, J.; Malayeri, A.; Rigamonti, D.; Lim, M.; Redmond, K.; Kleinberg, L. Postradiation imaging changes in the CNS: How can we differentiate between treatment effect and disease progression? *Future Oncol.* **2014**, *10*, 1277–1297. [\[CrossRef\]](#) [\[PubMed\]](#)
64. Galldiks, N.; Kocher, M.; Ceccon, G.; Werner, J.; Brunn, A.; Deckert, M.; Pope, W.; Soffietti, R.; Le Rhun, E.; Weller, M.; et al. Imaging challenges of immunotherapy and targeted therapy in patients with brain metastases: Response, progression, and pseudoprogression. *Neuro Oncol.* **2019**, *22*, 17–30. [\[CrossRef\]](#) [\[PubMed\]](#)
65. Tomura, N.; Kokubun, M.; Saginoya, T.; Mizuno, Y.; Kikuchi, Y. Differentiation between Treatment-Induced Necrosis and Recurrent Tumors in Patients with Metastatic Brain Tumors: Comparison among <sup>11</sup>C-Methionine-PET, FDG-PET, MR Permeability Imaging, and MRI-ADC-Preliminary Results. *Am. J. Neuroradiol.* **2017**, *38*, 1520–1527. [\[CrossRef\]](#)

66. Yomo, S.; Oguchi, K. Prospective study of  $^{11}\text{C}$ -methionine PET for distinguishing between recurrent brain metastases and radiation necrosis: Limitations of diagnostic accuracy and long-term results of salvage treatment. *BMC Cancer* **2017**, *17*, 713. [\[CrossRef\]](#)
67. Tsuyuguchi, N.; Sunada, I.; Iwai, Y.; Yamanaka, K.; Tanaka, K.; Takami, T.; Otsuka, Y.; Sakamoto, S.; Ohata, K.; Goto, T.; et al. Methionine positron emission tomography of recurrent metastatic brain tumor and radiation necrosis after stereotactic radiosurgery: Is a differential diagnosis possible? *J. Neurosurg.* **2003**, *98*, 1056–1064. [\[CrossRef\]](#)
68. Cicone, F.; Minniti, G.; Romano, A.; Papa, A.; Scaringi, C.; Tavanti, F.; Bozzao, A.; Maurizi Enrici, R.; Scopinaro, F. Accuracy of F-DOPA PET and perfusion-MRI for differentiating radionecrotic from progressive brain metastases after radiosurgery. *Eur. J. Nucl. Med. Mol. Imaging* **2014**, *42*, 103–111. [\[CrossRef\]](#)
69. Cicone, F.; Carideo, L.; Scaringi, C.; Romano, A.; Mamede, M.; Papa, A.; Tofani, A.; Cascini, G.; Bozzao, A.; Scopinaro, F.; et al. Long-term metabolic evolution of brain metastases with suspected radiation necrosis following stereotactic radiosurgery: Longitudinal assessment by F-DOPA PET. *Neuro Oncol.* **2020**, *23*, 1024–1034. [\[CrossRef\]](#)
70. Galldiks, N.; Stoffels, G.; Filss, C.; Piroth, M.; Sabel, M.; Ruge, M.; Herzog, H.; Shah, N.; Fink, G.; Coenen, H.; et al. Role of O-(2-(18F-fluoroethyl)-L-tyrosine PET for differentiation of local recurrent brain metastasis from radiation necrosis. *J. Nucl. Med.* **2012**, *53*, 1367–1374. [\[CrossRef\]](#)
71. Cecon, G.; Lohmann, P.; Stoffels, G.; Judov, N.; Filss, C.; Rapp, M.; Bauer, E.; Hamisch, C.; Ruge, M.; Kocher, M.; et al. Dynamic O-(2-18F-fluoroethyl)-L-tyrosine positron emission tomography differentiates brain metastasis recurrence from radiation injury after radiotherapy. *Neuro Oncol.* **2017**, *19*, 281–288. [\[PubMed\]](#)
72. Romagna, A.; Unterrainer, M.; Schmid-Tannwald, C.; Brendel, M.; Tonn, J.; Nachbichler, S.; Muacevic, A.; Bartenstein, P.; Kreth, F.; Albert, N. Suspected recurrence of brain metastases after focused high dose radiotherapy: Can [ $^{18}\text{F}$ ]FET- PET overcome diagnostic uncertainties? *Radiat. Oncol.* **2016**, *11*, 139. [\[CrossRef\]](#) [\[PubMed\]](#)
73. Galldiks, N.; Lohmann, P.; Albert, N.; Tonn, J.; Langen, K. Current status of PET imaging in neuro-oncology. *Neurooncol. Adv.* **2019**, *1*, 1–10. [\[CrossRef\]](#) [\[PubMed\]](#)
74. Bělohávek, O.; Šimonová, G.; Kantorová, I.; Novotný, J.; Liščák, R. Brain metastases after stereotactic radiosurgery using the Leksell gamma knife: Can FDG PET help to differentiate radionecrosis from tumour progression? *Eur. J. Nucl. Med. Mol. Imaging* **2003**, *30*, 96–100. [\[CrossRef\]](#)
75. Lai, G.; Mahadevan, A.; Hackney, D.; Warnke, P.; Nigim, F.; Kasper, E.; Wong, E.; Carter, B.; Chen, C. Diagnostic Accuracy of PET, SPECT, and Arterial Spin-Labeling in Differentiating Tumor Recurrence from Necrosis in Cerebral Metastasis after Stereotactic Radiosurgery. *Am. J. Neuroradiol.* **2015**, *36*, 2250–2255. [\[CrossRef\]](#) [\[PubMed\]](#)
76. Horky, L.; Hsiao, E.; Weiss, S.; Drappatz, J.; Gerbaudo, V. Dual phase FDG-PET imaging of brain metastases provides superior assessment of recurrence versus post-treatment necrosis. *J. Neurooncol.* **2010**, *103*, 137–146. [\[CrossRef\]](#)
77. Matuszak, J.; Waissi, W.; Clavier, J.B.; Noël, G.; Namer, I.J. Métastases cérébrales: Apport de l'acquisition tardive en TEP/TDM au 18F-FDG pour le diagnostic différentiel entre récurrence tumorale et radionécrose. *Méd. Nucl.* **2016**, *40*, 129–141. [\[CrossRef\]](#)
78. Silva, C.B.; Ongaratti, B.R.; Trott, G.; Haag, T.; Ferreira, N.P.; Leães, C.G.; Pereira-Lima, J.F.; Oliveira Mda, C. Expression of somatostatin receptors (SSTR1-SSTR5) in meningiomas and its clinicopathological significance. *Int. J. Clin. Exp. Pathol.* **2015**, *8*, 13185–13192.
79. Afshar-Oromieh, A.; Giesel, F.; Linhart, H.; Haberkorn, U.; Haufe, S.; Combs, S.; Podlesek, D.; Eisenhut, M.; Kratochwil, C. Detection of cranial meningiomas: Comparison of  $^{68}\text{Ga}$ -DOTATOC PET/CT and contrast-enhanced MRI. *Eur. J. Nucl. Med. Mol. Imaging* **2012**, *39*, 1409–1415. [\[CrossRef\]](#)
80. Galldiks, N.; Albert, N.; Sommerauer, M.; Grosu, A.; Ganswindt, U.; Law, I.; Preusser, M.; Le Rhun, E.; Vogelbaum, M.; Zadeh, G.; et al. PET imaging in patients with meningioma-report of the RANO/PET Group. *Neuro Oncol.* **2017**, *19*, 1576–1587. [\[CrossRef\]](#)
81. Farce, J.; Lecouillard, I.; Carsin Nicol, B.; Bretonnier, M.; Girard, A. Intracavernous Schwannoma Characterized With 18F-FDG,  $^{68}\text{Ga}$ -DOTATOC, and 18F-Choline PET. *Clin. Nucl. Med.* **2022**, *47*, e165–e166. [\[CrossRef\]](#)
82. Rachinger, W.; Stoecklein, V.; Terpolilli, N.; Haug, A.; Ertl, L.; Pöschl, J.; Schüller, U.; Schichor, C.; Thon, N.; Tonn, J. Increased  $^{68}\text{Ga}$ -DOTATATE uptake in PET imaging discriminates meningioma and tumor-free tissue. *J. Nucl. Med.* **2015**, *56*, 347–353. [\[CrossRef\]](#) [\[PubMed\]](#)
83. Milker-Zabel, S.; Zabel-du Bois, A.; Henze, M.; Huber, P.; Schulz-Ertner, D.; Hoess, A.; Haberkorn, U.; Debus, J. Improved target volume definition for fractionated stereotactic radiotherapy in patients with intracranial meningiomas by correlation of CT, MRI, and [ $^{68}\text{Ga}$ ]-DOTATOC-PET. *Int. J. Radiat. Oncol. Biol. Phys.* **2006**, *65*, 222–227. [\[CrossRef\]](#) [\[PubMed\]](#)
84. Henze, M.; Schuhmacher, J.; Hipp, P.; Kowalski, J.; Becker, D.W.; Doll, J.; Mäcke, H.R.; Hofmann, M.; Debus, J.; Haberkorn, U. PET imaging of somatostatin receptors using [ $^{68}\text{Ga}$ ]DOTA-D-Phe1-Tyr3-octreotide: First results in patients with meningiomas. *J. Nucl. Med.* **2001**, *42*, 1053–1056. [\[PubMed\]](#)
85. Klingenstein, A.; Haug, A.R.; Miller, C.; Hintschich, C. Ga-68-DOTA-TATE PET/CT for discrimination of tumors of the optic pathway. *Orbit* **2015**, *34*, 16–22. [\[CrossRef\]](#)



86. Graf, R.; Nyuyki, F.; Steffen, I.; Michel, R.; Fahdt, D.; Wust, P.; Brenner, W.; Budach, V.; Wurm, R.; Plotkin, M. Contribution of  $^{68}\text{Ga}$ -DOTATOC PET/CT to target volume delineation of skull base meningiomas treated with stereotactic radiation therapy. *Int. J. Radiat. Oncol. Biol. Phys.* **2013**, *85*, 68–73. [\[CrossRef\]](#) [\[PubMed\]](#)
87. Dittmar, J.; Kratochwil, C.; Dittmar, A.; Welzel, T.; Habermehl, D.; Rieken, S.; Giesel, F.; Haberkorn, U.; Debus, J.; Combs, S. First intraindividual comparison of contrast-enhanced MRI, FET- and DOTATOC- PET in patients with intracranial meningiomas. *Radiat. Oncol.* **2017**, *12*, 169. [\[CrossRef\]](#)
88. Gudjonsson, O.; Blomquist, E.; Lilja, A.; Ericson, H.; Bergström, M.; Nyberg, G. Evaluation of the effect of high-energy proton irradiation treatment on meningiomas by means of  $^{11}\text{C}$ -L-methionine PET. *Eur. J. Nucl. Med.* **2000**, *27*, 1793–1799. [\[CrossRef\]](#)
89. Ryttefors, M.; Danfors, T.; Latini, F.; Montelius, A.; Blomquist, E.; Gudjonsson, O. Long-Term evaluation of the effect of hypofractionated high-energy proton treatment of benign meningiomas by means of  $(^{11}\text{C})$ -L-methionine positron emission tomography. *Eur. J. Nucl. Med. Mol. Imaging* **2016**, *43*, 1432–1443. [\[CrossRef\]](#)
90. Kowalski, E.; Khairnar, R.; Gryaznov, A.; Kesari, V.; Koroulakis, A.; Raghavan, P.; Chen, W.; Woodworth, G.; Mishra, M.  $^{68}\text{Ga}$ -DOTATATE PET-CT as a tool for radiation planning and evaluating treatment responses in the clinical management of meningiomas. *Radiat. Oncol.* **2021**, *16*, 151. [\[CrossRef\]](#)
91. Mirimanoff, R.; Dosoretz, D.; Linggood, R.; Ojemann, R.; Martuza, R. Meningioma: Analysis of recurrence and progression following neurosurgical resection. *J. Neurosurg.* **1985**, *62*, 18–24. [\[CrossRef\]](#)
92. Kunz, W.; Jungblut, L.; Kazmierczak, P.; Vettermann, F.; Bollenbacher, A.; Tonn, J.; Schichor, C.; Rominger, A.; Albert, N.; Bartenstein, P.; et al. Improved Detection of Transosseous Meningiomas Using  $^{68}\text{Ga}$ -DOTATATE PET/CT Compared with Contrast-Enhanced MRI. *J. Nucl. Med.* **2017**, *58*, 1580–1587. [\[CrossRef\]](#)
93. Marincek, N.; Radojewski, P.; Dumont, R.; Brunner, P.; Müller-Brand, J.; Maecke, H.; Briel, M.; Walter, M. Somatostatin receptor-targeted radiopeptide therapy with  $^{90}\text{Y}$ -DOTATOC and  $^{177}\text{Lu}$ -DOTATOC in progressive meningioma: Long-term results of a phase II clinical trial. *J. Nucl. Med.* **2015**, *56*, 171–176. [\[CrossRef\]](#)
94. Seystahl, K.; Stoecklein, V.; Schüller, U.; Rushing, E.; Nicolas, G.; Schäfer, N.; Ilhan, H.; Pangalu, A.; Weller, M.; Tonn, J.; et al. Somatostatin receptor-targeted radionuclide therapy for progressive meningioma: Benefit linked to  $^{68}\text{Ga}$ -DOTATATE/-TOC uptake. *Neuro Oncol.* **2016**, *18*, 1538–1547. [\[CrossRef\]](#)
95. Muther, M.; Roll, W.; Brokinkel, B.; Zinnhardt, B.; Sporns, P.; Seifert, R.; Schäfers, M.; Weckesser, M.; Stegger, L.; Stummer, W.; et al. Response assessment of somatostatin receptor targeted radioligand therapies for progressive intracranial meningioma. *Nuklearmedizin* **2020**, *59*, 348–355. [\[CrossRef\]](#)
96. Yang, M.; Sun, J.; Bai, H.; Tao, Y.; Tang, X.; States, L.; Zhang, Z.; Zhou, J.; Farwell, M.; Zhang, P.; et al. Diagnostic accuracy of SPECT, PET, and MRS for primary central nervous system lymphoma in HIV patients: A systematic review and meta-analysis. *Medicine* **2017**, *96*, e6676. [\[CrossRef\]](#) [\[PubMed\]](#)
97. Hatakeyama, J.; Ono, T.; Takahashi, M.; Oda, M.; Shimizu, H. Differentiating between Primary Central Nervous System Lymphoma and Glioblastoma: The Diagnostic Value of Combining  $^{18}\text{F}$ -fluorodeoxyglucose Positron Emission Tomography with Arterial Spin Labeling. *Neurol. Med. Chir.* **2021**, *61*, 367–375. [\[CrossRef\]](#) [\[PubMed\]](#)
98. Bertaux, M.; Houillier, C.; Edeline, V.; Habert, M.; Mokhtari, K.; Giron, A.; Bergeret, S.; Hoang-Xuan, K.; Cassoux, N.; Touitou, V.; et al. Use of FDG-PET/CT for systemic assessment of suspected primary central nervous system lymphoma: A LOC study. *J. Neurooncol.* **2020**, *148*, 343–352. [\[CrossRef\]](#) [\[PubMed\]](#)
99. Park, H.Y.; Suh, C.H.; Huang, R.Y.; Guenette, J.P.; Kim, H.S. Diagnostic Yield of Body CT and Whole-Body FDG PET/CT for Initial Systemic Staging in Patients with Suspected Primary CNS Lymphoma: A Systematic Review and Meta-Analysis. *Am. J. Roentgenol.* **2021**, *216*, 1172–1182. [\[CrossRef\]](#)
100. Laudicella, R.; Quartuccio, N.; Argiroffi, G.; Alongi, P.; Baratto, L.; Califaretti, E.; Frantellizzi, V.; De Vincentis, G.; Del Sole, A.; Evangelista, L.; et al. Unconventional non-amino acidic PET radiotracers for molecular imaging in gliomas. *Eur. J. Nucl. Med. Mol. Imaging* **2021**, *48*, 3925–3939. [\[CrossRef\]](#)
101. Alongi, P.; Vetrano, I.G.; Fiasconaro, E.; Alaimo, V.; Laudicella, R.; Bellavia, M.; Rubino, F.; Bagnato, S.; Galardi, G. Choline-PET/CT in the Differential Diagnosis between Cystic Glioblastoma and Intraparenchymal Hemorrhage. *Curr. Radiopharm.* **2019**, *12*, 88–92. [\[CrossRef\]](#) [\[PubMed\]](#)
102. Deuschl, C.; Kirchner, J.; Poeppel, T.D.; Schaarschmidt, B.; Kebir, S.; El Hindy, N.; Hense, J.; Quick, H.H.; Glas, M.; Herrmann, K.; et al.  $(^{11}\text{C})$ -MET PET/MRI for detection of recurrent glioma. *Eur. J. Nucl. Med. Mol. Imaging* **2018**, *45*, 593–601. [\[CrossRef\]](#) [\[PubMed\]](#)
103. Afshar-Oromieh, A.; Wolf, M.B.; Kratochwil, C.; Giesel, F.L.; Combs, S.E.; Dimitrakopoulou-Strauss, A.; Gnirs, R.; Roethke, M.C.; Schlemmer, H.P.; Haberkorn, U. Comparison of  $^{68}\text{Ga}$ -DOTATOC-PET/CT and PET/MRI hybrid systems in patients with cranial meningioma: Initial results. *Neuro Oncol.* **2015**, *17*, 312–319. [\[CrossRef\]](#) [\[PubMed\]](#)
104. Brendle, C.; Maier, C.; Bender, B.; Schittenhelm, J.; Paulsen, F.; Renovanz, M.; Roder, C.; Castaneda-Vega, S.; Tabatabai, G.; Ernemann, U.; et al. Impact of  $^{18}\text{F}$ -FET PET/MR on clinical management of brain tumor patients. *J. Nucl. Med.* **2021**. [\[CrossRef\]](#)
105. Russo, G.; Stefano, A.; Alongi, P.; Comelli, A.; Catalfamo, B.; Mantarro, C.; Longo, C.; Altieri, R.; Certo, F.; Cosentino, S.; et al. Feasibility on the Use of Radiomics Features of  $^{11}\text{C}$ -MET PET/CT in Central Nervous System Tumours: Preliminary Results on Potential Grading Discrimination Using a Machine Learning Model. *Curr. Oncol.* **2021**, *28*, 5318–5331. [\[CrossRef\]](#)

- 
106. Kebir, S.; Rauschenbach, L.; Weber, M.; Lazaridis, L.; Schmidt, T.; Keyvani, K.; Schäfer, N.; Milia, A.; Umutlu, L.; Pierscianek, D.; et al. Machine learning-based differentiation between multiple sclerosis and glioma WHO II°–IV° using O-(2-[18F] fluoroethyl)-L-tyrosine positron emission tomography. *J. Neuro-Oncol.* **2021**, *152*, 325–332. [[CrossRef](#)]
  107. Qian, J.; Herman, M.G.; Brinkmann, D.H.; Laack, N.N.; Kemp, B.J.; Hunt, C.H.; Lowe, V.; Pafundi, D.H. Prediction of MGMT Status for Glioblastoma Patients Using Radiomics Feature Extraction From 18F-DOPA-PET Imaging. *Int. J. Radiat. Oncol. Biol. Phys.* **2020**, *108*, 1339–1346. [[CrossRef](#)]